

11-28-2018

A Two Compartment Pharmacokinetic Model Describes the Intra-articular Delivery and Retention of rhPRG4 Following ACL Transection in the Yucatan Mini Pig

Mark Hurtig
University of Guelph

Iman Zaghoul
Massachusetts College of Pharmacy & Health Science

Heather Sheardown
McMaster University

Tannin A. Schmidt
University of Connecticut

Lina Liu
McMaster University

See next page for additional authors
View this and additional works at: https://digitalcommons.chapman.edu/pharmacy_articles



Part of the [Animal Experimentation and Research Commons](#), [Animals Commons](#), [Medicinal and Pharmaceutical Chemistry Commons](#), and the [Other Pharmacy and Pharmaceutical Sciences Commons](#)

Recommended Citation

Hurtig M, Zaghoul I, Sheardown H, et al. A two compartment pharmacokinetic model describes the intra-articular delivery and retention of rhPRG4 following ACL transection in the Yucatan mini pig. *J Orthop Res.* 2018;37(2):386-396. doi: 10.1002/jor.24191

This Article is brought to you for free and open access by the School of Pharmacy at Chapman University Digital Commons. It has been accepted for inclusion in Pharmacy Faculty Articles and Research by an authorized administrator of Chapman University Digital Commons. For more information, please contact laughtin@chapman.edu.

A Two Compartment Pharmacokinetic Model Describes the Intra-articular Delivery and Retention of rhPRG4 Following ACL Transection in the Yucatan Mini Pig

Comments

This is the accepted version of the following article:

Hurtig M, Zaghoul I, Sheardown H, et al. A two compartment pharmacokinetic model describes the intra-articular delivery and retention of rhPRG4 following ACL transection in the Yucatan mini pig. *J Orthop Res.* 2018;37(2):386-396. doi: 10.1002/jor.24191

which has been published in final form at DOI: [10.1002/jor.24191](https://doi.org/10.1002/jor.24191). This article may be used for non-commercial purposes in accordance with [Wiley Terms and Conditions for Self-Archiving](#).

Copyright

Wiley

Authors

Mark Hurtig, Iman Zaghoul, Heather Sheardown, Tannin A. Schmidt, Lina Liu, Ling Zhang, Khaled A. Elsaid, and Gregory D. Jay

Research Article

**A Two Compartment Pharmacokinetic Model Describes the Intra-articular
Delivery and Retention of rhPRG4 Following ACL Transection in the
Yucatan Mini Pig[†]**

Running Title: Lubricin (rhPRG4) Pharmacokinetics

Mark Hurtig DVM¹

Iman Zaghoul PhD²

Heather Sheardown PhD³

Tannin A. Schmidt PhD^{4,5}

Lina Liu MS³

Ling Zhang MD⁶

Khaled A. Elsaid Pharm.D., PhD⁷

Gregory D. Jay MD-PhD^{6,8}

¹Ontario Veterinary College, University of Guelph, Guelph, ON, Canada

²Department of Pharmaceutical Sciences, Massachusetts College of Pharmacy and Health Sciences, Boston, MA, USA

³Department of Chemical Engineering, McMaster University, Hamilton, ON, Canada

⁴School of Dental Medicine, University of Connecticut Health Center, Farmington, CT, USA

⁵Biomedical Engineering Department, University of Connecticut Health Center, Farmington, CT, USA

⁶Department of Emergency Medicine, Warren Alpert Medical School, Brown University, Providence, RI, USA

⁷Department of Biomedical and Pharmaceutical Sciences, Chapman University School of Pharmacy, Irvine, CA, USA

⁸Division of Biomedical Engineering, School of Engineering at Brown University, Providence, RI, USA

[†]This article has been accepted for publication and undergone full peer review but has not been through the copyediting, typesetting, pagination and proofreading process, which may lead to differences between this version and the Version of Record. Please cite this article as doi: [10.1002/jor.24191]

Received 13 December 2017; Revised 24 August 2018; Accepted 3 October 2018

Journal of Orthopaedic Research®

This article is protected by copyright. All rights reserved

DOI 10.1002/jor.24191

Address for Correspondence: Gregory D. Jay MD-PhD, Department of Emergency Medicine Laboratory, 1 Hoppin Street, Coro West Suite 112, Rhode Island Hospital, Providence, RI 02903.

gregory_jay_md@brown.edu

Author Contributions: H.S., M.H., G.J. and K.E. conceived and designed the experiments; H.S., L.L., T.S. and G.J. prepared test articles; H.S., L.L., L.Z. and M.H. performed the experiments; I.Z., K.E. and G.J. analyzed the data; G.J. M.H., H.S., I.Z, K.E., T.S., L.Z. and L.L. wrote the paper.

Abstract Word Count: 248

Manuscript Word Count: 4200 without reference numbers

Funding: R01AR067748, R42AR057276, PR110746

Abstract

Treatment of the injured joint with rhPRG4 is based on recent observations that inflammation diminishes expression of native PRG4. Re-establishing lubrication between pressurized and sliding cartilage surfaces during locomotion promotes the nascent expression of PRG4 and thus intra-articular (IA) treatment strategies should be supported by pharmacokinetic evidence establishing the residence time of rhPRG4. A total of 21 Yucatan minipigs weighing ~55 Kg each received 4 mg of ^{131}I -rhPRG4 delivered by IA injection 5 days following surgical ACL transection. Animals were sequentially euthanized following IA rhPRG4 at 10 mins (time zero), 24, 72 hrs, 6, 13 and 20 days later. The decay of the ^{131}I -rhPRG4 was measured relative to a non-injected aliquot and normalized to the weight of cartilage samples, menisci and synovium, and known cartilage volumes from each compartment surface obtained from representative Yucatan minipig knees. Decay of ^{131}I -rhPRG4 from joint tissues best fit a two-compartment model with an α half-life ($t_{1/2\alpha}$) of 11.28 hours and β half-life ($t_{1/2\beta}$) of 4.81 days. The tibial and femoral cartilage, meniscii and synovium retained 7.7% of dose at 24 hrs. High concentrations of rhPRG4 were found in synovial fluid (SF) that was non-aspiratable and resided on the articular surfaces, removable by irrigation, at 10 mins following ^{131}I -rhPRG4 injection. Synovial fluid K21 exceeded K12 and SF $t_{1/2\beta}$ was 28 days indicating SF is the reservoir for rhPRG4 following IA injection. **Clinical Significance:** rhPRG4 following IA delivery in a traumatized joint populates articular surfaces for a considerable period and may promote the native expression of PRG4. This article is protected by copyright. All rights reserved

Keywords: Lubricin, PRG4, Pharmacokinetics, Half-life, Cartilage, Joint, ACL Transection

Introduction

Osteoarthritis (OA) ¹leads to functional disability and a reduced quality of life².

Abnormal biomechanics is a major risk factor in disease progression and joint tissue damage³.

Post-traumatic osteoarthritis (PTOA) is a syndrome of joint degeneration and pain that develops after joint injuries^{4; 5}. Treating joint pain alone may actually exacerbate PTOA^{7; 8} since the pain response is adaptively interfering with locomotion, and unloading the affected joint. New therapeutic approaches that mitigate the risk of developing PTOA, particularly for young patients with meniscal and anterior cruciate ligament (ACL) tears⁶ are needed.

Five different research groups have tested native⁹, recombinant human lubricin (rhPRG4)¹⁰⁻¹² or lubricin mimic biomolecules^{13; 14} by re-introducing these into rodent joints after injury in the effort to retard cartilage loss. The inflammation associated with meniscal and ACL injuries is thought to downregulate PRG4 expression^{15; 16}. Rats that underwent medial meniscectomy¹¹ or ACL transection^{9; 17} treated with repeated or single dose intra-articular (IA) rhPRG4¹⁰ showed a chondroprotective effects measured by improved histology. Two studies showed a reduction in urine levels of CTX-II—a classical biomarker of cartilage degradation^{10; 17}. Another study in ACL transected rat knees showed an improvement in the radiographic outcome following supplementation with lubricin¹⁸. Chondroprotective results were also evident in rats that underwent forced exercise¹⁷ and in mice where a helper-dependent adeno viral vector expressing *Prg4* prevented development of PTOA in mice¹⁹. Most recently we showed in large animals following destabilization of the medial meniscus (DMM)¹² that chondral lesions were smaller and synovial fluid (SF) CTX-II levels were significantly lower, 5.5 months later following IA rhPRG4. Lubricin supplementation decreases the number of apoptotic chondrocytes^{17; 20; 21} and increases

native lubricin expression¹⁰. Elevated joint friction in *Prg4* null mice²² also showed diminished chondrocyte density²³. A concern about lubricin supplementation is whether rhPRG4 has a favorable pharmacokinetic profile that would lead to its continued presence and enable tribological protection.

The half-life of radiolabeled truncated lubricin is 4.5 hours in a medial meniscectomized rat²⁴. However, this value must be reconciled with radioactivity still present on the articular surface up to 28 days following IA injection. Lubricin persists in traumatized cartilage²⁵ and contributes to protect joints from mechanical injury and may mitigate PTOA. Our current focus is to gather data in a large animal model, particularly at early time points in an injury model, to enable pharmacokinetic modeling that will be predictive of lubricin residence time in the human knee by allometric scaling²⁶. Transection of the ACL was chosen in a large animal model in this study since lubricin levels in patients with an untreated ACL injury require a year to return to normal²⁷ and leads to an aggressive PTOA, dependent on early alterations in the cartilage matrix²⁸.

METHODS

Animals

The study was conducted at University of Guelph, Ontario, Canada and used purpose-bred castrated male and female Yucatan mini-pigs (N=21) weighing 50-60 kg. All porcine were adolescent animals, born within 2 weeks of each other and were 9 months old at study conclusion. Each animal underwent hematological, physical and musculoskeletal examinations upon arrival from S&S Farms (Ramona, CA). Seven (7) days were permitted for acclimatization prior to

surgery during which the animals were housed in pairs or small groups depending on behavior. Animals were maintained in controlled environmental facilities at 20°C and light/dark cycle determined by ambient lighting. The study protocol was approved by the institutional animal care and use committee and conducted in accordance with the Canadian Council on Animal Care guidelines.

Manufacture of rhPRG4

The expression of rhPRG4 by CHO-M cells has been described previously²⁹. CHO-M cells were transfected with the full-length human PRG4 gene resulting in a 1404 amino acid PRG4 (Lubris, LLC, Framingham, MA). Manufacturing was performed by Peregrine Pharmaceuticals, Inc., Tustin, CA) under pre-GMP conditions. The presence of O-linked glycosylations comprised of (β1,3)Gal-GalNAc was previously confirmed by Western blot^{30; 31} and concentration was established by ELISA³¹.

Labelling of rhPRG4 with ¹³¹I

rhPRG4 was radiolabelled with ¹³¹I in 0.1M NaOH (Perkin Elmer Health Science, Canada, Inc) using the iodine monochloride method. Radiolabelled rhPRG4 was passed through a column containing AG1-X4 resin (Bio-Rad, Hercules, CA) to remove free ¹³¹I. The trichloroacetic acid test was performed to determine unbound ¹³¹I in the solution which did not exceed 8% (w/w). Vials containing 4 mg of ¹³¹I-rhPRG4 in 3 ml PBS carrier with 32 μCi radioactivity were prepared for animal injection.

Surgical and Anesthesia Procedures

Using general anesthesia and aseptic technique mini-pigs underwent arthroscopic ACL ligament transection of the right knee joint followed by the IA administration of 4 mg of ^{131}I -rhPRG4 5 days later. At the time of arthroscopy joint cavity irrigation was limited to 120 ml of sterile physiologic saline. Radiolabeling of rhPRG4 (Lubris, LLC) was performed at McMaster University, and sent the same day by courier to Ontario Veterinary College, University of Guelph. The ^{131}I -rhPRG4 was used within the day of arrival. The left knee was unaffected. There were no uninjected surgical control animals.

On the day of the surgery porcine were pre-medicated with acepromazine (0.2 mg/kg), atropine (0.05 mg/kg) and buprenorphine (0.02 mg/kg) given intramuscularly (IM). Anaesthesia was induced with ketamine (20 mg/kg) and mask-ventilated (or intubated with an endotracheal tube) with a 2% isoflurane O₂ mixture. Aspiration of SF from both knees was attempted prior to surgical entry of the joint. Postoperative analgesia consisted of peri-articular subcutaneous (sc) injection of diluted bupivacaine (0.25%, 0.05-0.1 mL, dose < 1 mg/kg) and sc buprenorphine (0.05 to 0.1 mg/kg) every 4-6 hours as needed for up to 72 hours.

On day 5 post-surgery (designated D=0) all 21 pigs were sedated with acepromazine (0.2 mg/kg) and ketamine (20 mg/kg) given IM to induce dissociative anesthesia, followed by an IA injection of 4 mg ^{131}I -rhPRG4 into the right knee. Flexion and extension of the right knee was performed for 5 minutes post injection to ensure distribution of the ^{131}I -rhPRG4.

Tissue Harvesting and Preparation of Counting for Radioactivity Decay

Minipigs were euthanized at specific timepoints determined *a priori* illustrated in Fig 1 for collection of tissues. Animals were euthanized by sedation with acepromazine and ketamine (as above) followed by an overdose of pentobarbitol (100 mg/kg) IV via an ear vein. Right knees were collected and SF was collected by aspiration. Upon gross dissection, cartilage surface irrigation with 5 ml of PBS was performed and recovered. Partial thickness cartilage specimens were excised from the medial femoral, medial tibial, lateral femoral, lateral tibial and patellar surfaces. The medial and lateral menisci were collected. Anterior and posterior synovial lining tissue, the pre-femoral lymph node, liver tissue and urine was also collected. Each of these tissues were weighed, and then held at 4 °C while transported to McMaster University for gamma counting within 3 hours of collection. A 24 hour urine collection was not conducted since metabolic cages were not available.

Gamma Counting

The amount of ¹³¹I-rhPRG4 remaining in tissues was measured using a Wizard 3 1480 Automatic Gamma Counter (Perkin Elmer, Woodbridge, ON, Canada). The gamma radiation counts were then converted to rhPRG4 amounts based on the counts of a non-injected ¹³¹I-rhPRG4 standard solution that was stored at McMaster University.

Prior Yucatan Minipig Cartilage, Meniscus and Synovium Total Mass Measurements

Four previously frozen unoperated Yucatan mini-pig left knee joints were disarticulated into separate segments that included the distal femur, proximal tibia and patella. The entire joint capsule was kept attached to the patella for subsequent soft tissue studies. The medial and lateral

menisci were excised and weighed using an analytical balance. A GE eXplore Locus CT scanner (Schenectady, NY) was used to image the bone and soft tissue segments in humidified air. An 18 minute long 45 micron resolution protocol³² resulted in 720 slices comprised of isotropic voxels. Slices were compiled and subsequently realigned in a true frontal plane. Image manipulation and analysis was done using Microview 2.5 (Parallax Innovations, Ilderton, ON, Canada). Articular cartilage volume and surface area were measured by outlining cartilage in thresholded frontal plane image slices using the advanced region of interest (ROI) (spline) tool. Three-dimensional ROIs were compiled and voxel counts from isosurface projections were used in calculation of area and volume (Figure 2). Separate ROIs were created for the medial and lateral condyles, medial and lateral tibial plateaus and patella cartilage plates. Cartilage mass was calculated by volume x 1.1 gm/cc based on volume displacement trials of porcine articular cartilage.

Synovial membrane mass was calculated by first identifying the geographic distribution of synovial membrane in normal mini-pig knees as determined by microCT imaging of the entire Lugol's iodine-stained joint capsule in Ringer's solution. Synovial tissue mass was determined from harvested normal unoperated joints by dissecting synovial fronds from the underlying joint capsule while the tissue was immersed in Ringer's solution which allowed the synovial tissue to float and adopt a three-dimensional villus profile. Areas of synovial lining tissue were weighed after collection using an operating microscope and micro-instruments.

Pharmacokinetic Calculations

The individual knee tissue concentrations of total radioactivity were normalized to a gram of tissue and the total amount of rhPRG4 per tissue was calculated using the total mass of individual knee tissues. The percent of rhPRG4 dose detected at each time point: zero (10 mins), 24, 72 hrs, 6, 13 and 20 days was calculated after a single IA dose of ^{131}I -rhPRG4 of 4 mg/knee. The area under the blood concentration-time curves (AUC) was calculated using the trapezoidal rule up to the last measured concentration, C_{last} . To the latter AUC was added C_{last}/β to calculate $\text{AUC}_{0-\infty}$. The parameters were determined for each individual animal and their average was calculated.

The total radioactivity counts of ^{131}I -rhPRG4 (expressed as percent of total dose) at each time point was calculated and fitted to two compartment model using Phoenix WnNonlin version 64 (Pharsight Corporation, Sunnyvale, CA, USA). The percent of total dose in cartilage, menisci and synovium at different time points were fitted using least square regression with either $1/y$ or $1/y^2$ weighting factors to two compartmental model ($C_t = Ae^{-\alpha t} + Be^{-\beta t}$) where C_t counts (as % dose) at time t were weighted as the inverse of the C_t . Pharmacokinetics parameters of blood concentrations of ^{131}I -rhPRG4 (μg equivalent/mL) at each time point were calculated for each individual animal after fitting the concentrations time curve to a two compartment model.

Western Blotting of PRG4 in SF and Joint Lavage Samples, and IL-1 β ELISA

SDS-PAGE electrophoresis of undiluted samples on pre-cast 4-12% gradient gels (ThermoFisher Scientific, Waltham, MA) and transfer to nitrocellulose was performed as described previously³¹.

Polyclonal antibody 1752 (ABPRO, Woburn, MA, USA) that reacts with the epitope

FESFERGRECDCAQCKKYDK in the N-terminus of PRG4³³ was used at 1:1000 dilution with 5% bovine serum albumin in PBST. Membranes were incubated with IRDye goat anti-

rabbit IgG at 1:10,000 dilution for 1 hr at RT with shaking. Levels of IL-1 β were measured on undiluted samples using a commercially available kit #PLB00B (R&D Systems, Minneapolis, MN).

Blot Imaging and Densitometric Analysis

The blots were imaged with LI-COR Odyssey (LI-COR Biosciences, Lincoln, NE, USA) imaging system with 800 or 700 CW according to manufacturer's instruction. NIH image J (<https://imagej.nih.gov/ij/>) was used for chemiluminescent band analysis (NIH, Bethesda, MD, USA). Lanes were compared to a β -actin standard and densitometrically normalized to a LI-COR anti- β actin monoclonal antibody #926-42210. Densitometric standards were established by imaging known amounts of rhPRG4 solubilized in normal porcine SF in different lanes of a blot simultaneously. The detectable limit of rhPRG4 concentration was 10 μ g/ml.

Tissue Processing and Immunohistochemistry

Following gamma counting at the time of sacrifice, all knee joint tissues were fixed in 10% formalin (PROTOCOLTM, Fisher, Waltham, MA, USA). After 4 months to allow for sufficient radioactive decay, samples were transported under United States Department of Agriculture permit #132894. Samples were decalcified using 0.48 M EDTA, with adjusted pH of 7.1 with ammonium hydroxide at 4°C. Embedded tissues were sectioned with a thickness of 10 μ m.

Sections were probed for surface accumulation and nascent expression of PRG4 within chondrocytes using monoclonal antibody 9G3³¹ (EMD Millipore; Darmstadt, Germany) which reacts with the mucin domain of PRG4 using methods described previously²⁵.

Statistical Methods

Data were reported as mean \pm standard deviation (SD) unless otherwise indicated. Descriptive statistical analyses were performed using Prism 6 software (GraphPad, La Jolla, CA).

RESULTS

Study Conduct and Tissue Recovery

This uncontrolled study was conducted over 16 months in groups of 6, 12 and 3 porcine due to animal availability. No adverse events occurred. Three animals were removed from the analysis since they evidently did not receive IA rhPRG4 since radioactivity was undetected in the SF from euthanized animals #39 and #91 at time point 10 minutes (time zero) and animal #86 at 24 hrs. In these animals, the principal radioactivity was recovered in either the proximal lymph node or in the urine. Across the remaining 18 porcine at the time point of 10 mins, an average of 32.0% of dose was located in the cartilage and synovial knee tissues, 20.7% in synovial fluid, 1.2% on the ACL stump, 0.09% in the proximal lymph node, 9.5% in liver and 35.4% in the lavage of the joint surfaces. Another lavage at 24 hrs only recovered 0.064% of dose suggesting that a majority of the rhPRG4 was present in the SF or fully adherent to articular and synovial surfaces. rhPRG4 was primarily excreted in the urine and was not significantly present in adjacent lymph nodes in the 18 animals that received the IA injection correctly. Tissue recoveries were not conducted for the first group of 6 animals allocated to time points 6,13 and 20 days post IA injection.

Elimination of I¹³¹-rhPRG4 and Akaike Information Criterion (AIC) model fitting

Figure 3a shows the distribution and elimination of the percent dose of total radioactivity of the knee which included all joint tissues, the lavage fluid and SF which in aggregate accounted for 89.4% of total dose. At 24 hrs after injection, 7.7% of the total instilled dose of ¹³¹I-rhPRG4 is resident in the joint. Radioactivity is still present on days 13 and 20 suggesting that the complete elimination of ¹³¹I-rhPRG4 is delayed. A two-compartment elimination model, using AIC, best fit these data from the 18 porcine using counts from cartilage, meniscii and synovial tissue which accounted for 33% of dose (Figure 3b). The porcine knee joint modeled with this two-compartment elimination model shows that the α half-life ($t_{1/2\alpha}$) phase is 11.28 hours and the $t_{1/2\beta}$ is 4.81 days long (Figure 3c and 3d).

Different modeling permutations of tissue counts from cartilage, meniscii and synovium, SF and cartilage surface lavage were analyzed in Table 1 to identify tissues and/or fluids with maximal $t_{1/2\alpha}$ and $t_{1/2\beta}$. Permutations that included counts from cartilage lavage had a shorter $t_{1/2\beta}$ and did not appear different than those containing cartilage tissues. Table 1 also indicates that $t_{1/2\alpha}$ and $t_{1/2\beta}$ values did not lengthen when considering only counts from cartilage, meniscii and synovial tissue. Permutations that included SF counts maximized $t_{1/2\beta}$ to a maximal time of 28 days.

Calculation of K12 and K21 (Table 1) for cartilage, meniscii, synovial tissues and SF shows that $K21 > K12$ for SF and synovium indicating that ¹³¹I-rhPRG4 was more likely to reside in SF or on synovial surfaces. Cartilage and other tissues, with and without lavage all showed $K21 < K12$ indicating that ¹³¹I-rhPRG4 was more likely retained on cartilage and meniscii. The long SF $t_{1/2\beta}$ value of 28 days and the $K21/K12$ ratio greater than unity support that SF is the reservoir for PRG4.

The blood concentrations of total radioactivity of ^{131}I -rhPRG4 also showed a two-compartment profile with the highest concentrations shown at 10 minutes after dose ($5.8\pm 7.1\ \mu\text{g}$ equivalent/mL). Lubricin was eliminated from the systemic circulation with a mean total clearance of $21.54\pm 4.18\ \text{mL/day/kg}$ and a $t_{1/2\alpha}$ of 6.48 hours and $t_{1/2\beta}$ of 15.88 days. However, the mean systemic exposure represented by total area under the blood concentrations time curve ($\text{AUC}_{0-\infty}$) was $< 15\%$ of the total area under the knee tissue concentrations curve of ^{131}I -rhPRG4 (3.38 ± 0.65 vs $26.32\pm 0.47\ \mu\text{g}$ equivalent day/mL). Following the IA administration of ^{131}I -rhPRG4 9.5% of total dose was found in the liver after 10 mins which decreased to 5.6% and 0.36% after 1 and 13 days, respectively. However, no radioactivity was detected on day 20.

Tibial-femoral Joint Compartmentalization of rhPRG4

Tibial cartilage and synovial membrane surfaces appeared to contain relatively larger amounts of ^{131}I -rhPRG4 at time 0 (Figure 4a). By day 1 synovial surfaces appeared to contain relatively larger amounts of ^{131}I -rhPRG4. By day 13 and 20, cartilage surfaces showed the greatest relative amounts of ^{131}I -rhPRG4 (Figure 4b). In comparing the proportion of ^{131}I -rhPRG4 localizing to the femoral and tibial cartilage in medial and lateral joint compartments we observed that initially ^{131}I -rhPRG4 localized more to the tibial cartilage surfaces and equally to both tibiofemoral joint compartments (Figure 5a). Towards the end of the concentration-time profiles studied at day 20, the lateral joint compartment and femoral cartilage retained a greater relative percentage of recoverable ^{131}I -rhPRG4 (Figure 5b).

Cartilage Surface Lavage and Western Blots of rhPRG4 and Porcine PRG4

Both rhPRG4 and native porcine PRG4 were detected on Western blots of recovered cartilage surface lavages (Figure 6a). The different molecular weights of detectable rhPRG4 (apparent MW~300 kDa) and porcine PRG4 (MW~180 Kda) enabled the densitometric measurement of rhPRG4 relative to porcine PRG4. Figure 6a shows that rhPRG4 was detectable up to 13 days after IA injection. Semi-quantitative analysis in Figure 6b indicates that rhPRG4 levels are initially high at time zero, decreased at 24-72 hrs, and were near zero by day 20. By contrast, the relative amounts of porcine PRG4 increased from day 3 to day 13.

Immunohistochemistry of Total PRG4, and IL-1 β Levels

The observation that the amount of rhPRG4 was decreasing as the relative amount of native PRG4 increased is supported by immunohistochemistry using mAb 9G3 for total PRG4 on the articular surfaces (Figure 7). The total detectable amount of surface PRG4 diminished from day 1 to day 20. Near the time of IA delivery at 10 minutes there is some immunoreactivity at the articular surface but significantly less than cartilage from animals sacrificed after 24 hours likely indicating that sometime was needed for rhPRG4 to interact with the articular surface and colocalize with native porcine PRG4. Superficial zone chondrocyte immunopositivity for PRG4 became more observable at days 6 and 13 suggesting that endogenous production of porcine PRG4 was increased during the time course of the study. IL-1 β at time 0 in surface lavage was 319.8 ± 365.8 pg/ml (N=3) and 74.8 ± 81.8 pg/ml in SF (N=3). At 24 hrs two porcine had SF levels of 88.7 and 34.8 pg/ml. IL-1 β levels were below detectable limits for porcine SF and lavaged samples over the remaining time points with the exception of 34.1 pg/ml for a SF sample at 20 days.

DISCUSSION

Recombinant human PRG4 is surface active and recapitulates the ability of natural lubricin to coat biological surfaces and provide both anti-adhesive³⁴⁻³⁶ and lubricating activity²⁹. Lubricin forms end-grafted brushes³⁷⁻³⁹ that provide steric hindrance against a like-covered apposing articular surface and structures hydration shells vis-à-vis extensive O-linked glycosylations^{40; 41} that exist in the mucin domain. Lubricin interacts with biological and non-biological surfaces, and has a preponderance to interact with hydrophobic surfaces^{42; 43}. The results support a partitioning of lubricin that is cartilage bound and unbound within the SF. Partitioning provides a reservoir of lubricin⁴⁴ that can replace lubricin that is sacrificially worn away during articulation⁴⁵. This is supported by the high amounts of ¹³¹I-rhPRG4 recovered from cartilage surfaces with irrigation soon after IA delivery, and from SF recovered from closed joint needle aspiration; suggesting that ¹³¹I-rhPRG4 was tethered but not fully adherent to the cartilage surface. These observations support the two-compartment pharmacokinetic elimination model. The $t_{1/2\alpha}$ of 11.28 hrs reflects rhPRG4 that is primarily metabolized in SF which is contained within the diarthrodial joint structure. Comparatively less radiolabel was detected in the blood, liver, urine or proximal lymph node after IA injection. The $t_{1/2\beta}$ of 4.81 days is reflective of lubricin that was likely cartilage, meniscii and synovial surface bound. These estimates are driven by the tissues only model in Fig 3b which accounted for 33% of total radioactivity. Both half-lives are in fair agreement with a prior effort²⁴ in medial meniscectomized rat knees that were injected with ¹³¹I-truncated rhPRG4 3 weeks later. In that study, a three-compartment model best fit the PRG4 concentration-time profiles and reported α , β and γ half-life estimates of 4.5 hrs, 1.5 days and 2.1 weeks respectively. We were unable to fit a three compartment model with our data which may be due to lack of sampling times past 20 days. Considering counts from the SF exclusively lengthened $t_{1/2\beta}$ to 28

days which is in agreement with the earlier rat study²⁴. The long $t_{1/2\beta}$ in SF and the fact that K21 > K12 (Table 1) suggests that SF is the reservoir for PRG4 and that rhPRG4 may emulate its biophysical and physisorptive activity.

In comparing these two studies it is important to realize that the present effort used a larger joint and a full-length recombinant human lubricin that was 1404 amino acids long which may have a longer residence time. The present study was accomplished with an arthroscope to transect the ACL ligament, thus reducing tissue injury associated with an arthrotomy. Use of a minimally invasive surgical technique, and delay in treatment, are approaches that recapitulate current clinical practice. We also observed in Figs 4-5 that the tibial cartilage surfaces showed a disproportionate loss of rhPRG4 over time compared to the femoral cartilage. Since cartilage thinning following ACL injury is predicted to be more severe in tibial cartilage and in the medial compartment⁴⁶, we posit if friction-induced metabolic changes in cartilage can confound rhPRG4, PRG4⁴⁷ and Prg4⁴⁸ in serving its chondroprotective role.

The introduction of rhPRG4 into an injured joint may have several positive consequences. Local PRG4 expression is upregulated by physical activity⁴⁹. The combination of compression and shear *in vitro* has been observed to increase expression of PRG4 by several laboratories^{45; 50; 51}. Human recombinant PRG4 also displays anti-inflammatory properties through inhibition of the innate immunity receptors, TLR2 and TLR4^{52; 53}. Suppressing inflammation by itself may play a positive role since incubation of bovine cartilage explants with IL-1 β *in vitro* has been shown to suppress native PRG4 expression²⁵. Figures 6 and 7 together support the notion that rhPRG4 densely coated cartilage surfaces on days 1 and 3 post injection and subsequently diminished over time. Some of

the rhPRG4 may have penetrated into the cartilage²⁵ which is supported by the continued radioactivity of cartilage despite surface irrigation. By post-injection days 6 and 13 resident porcine chondrocyte PRG4 expression was qualitatively supported by chondrocyte immunoreactivity (Figure 7). We posit that the presence of rhPRG4 served to restore the expression of native PRG4 in an inflammatory environment that was down trending as a result of the ACL transection surgery 5 days previous.

The cartilage surface area of the human knee is 121 cm²⁵⁴ and 277 cm²⁵⁵ for the synovium. The cartilage surface area in the Yucatan mini-pig was 32.4 cm². Availability for rhPRG4 binding is thus allometrically 3.7 times larger in the human joint. The 4 mg dose used in the present study was effective in mitigating PTOA in the same porcine species following DMM when used weekly over three weeks¹². A dose escalated single injection study is planned and supported by a recent study in the rat where a single 260 µg/kg IA rhPRG4 dose, was equally effective to smaller repetitive doses¹⁰. Extrapolating the distribution of availability based on cartilage surface area alone in the human knee from the mini-pig knee leads to the conclusion that a 14.8 mg dose of rhPRG4 provided shortly after an acute knee injury may be enough to achieve both cartilage surface coverage and bioavailability from SF. This calculation does not consider the much larger synovial membrane area. The synovium demonstrated considerable radioactive counts suggesting that rhPRG4 was present. Uptake of biomaterials and biologics occurs across synovial villi²⁶, and is a source of PRG4 synthesis⁵⁶ that is under autoregulation⁵². The present study did not involve HA to take advantage of possible synergistic effects with PRG4^{18; 30; 57-60}. We observed immunopositivity for PRG4 only in the synovium at time 0 (data not shown) but in the absence of a non-injected surgical control animal we cannot conclude if this represents a lack of porcine PRG4

contribution from the synovium.

Limitations include the application of rhPRG4 early in a PTOA animal model in which disease progression was not studied histologically. A relatively low amount of joint cavity irrigation was used during arthroscopy. Irrigation has been shown to eliminate the resident lubricin in the bovine joint⁶¹. The lower amounts of irrigation used for this surgical injury may have resulted in the rhPRG4 mixing with resident porcine PRG4 which could impact its bioavailability. By contrast, 5 days after surgery also likely diminished resident porcine PRG4 levels²⁵. However, an increase in native PRG4 expression from the synovium as observed in an equine OA model, 20 days following surgery⁶² has not been excluded. Our study was conducted cumulatively across 3 groups of animals due to logistical challenges. Tissues that were recovered in the first group were not retained for later histological analysis; a limitation corrected for most of the animals. Finally, this study was conducted in quadrupeds that have a different gait pattern than humans and were not skeletally mature. However, ACL transection recapitulates a common joint injury in adolescent humans.

References

1. Lawrence RC, Felson DT, Helmick CG, et al. 2008. Estimates of the prevalence of arthritis and other rheumatic conditions in the United States. Part II. *Arthritis Rheum* 58:26-35.
2. Hunter DJ, McDougall JJ, Keefe FJ. 2008. The symptoms of osteoarthritis and the genesis of pain. *Rheum Dis Clin North Am* 34:623-643.
3. Block JA, Shakoor N. 2009. The biomechanics of osteoarthritis: implications for therapy. *Curr Rheumatol Rep* 11:15-22.
4. Anderson DD, Chubinskaya S, Guilak F, et al. 2011. Post-traumatic osteoarthritis: Improved understanding and opportunities for early intervention. *J Orthop Res* 29:802-809.
5. Buckwalter JA, Brown TD. 2004. Joint injury, repair, and remodeling: roles in post-traumatic osteoarthritis. *Clin Orthop Relat Res*:7-16.
6. Suter LG, Smith SR, Katz JN, et al. 2017. Projecting Lifetime Risk of Symptomatic Knee Osteoarthritis and Total Knee Replacement in Individuals Sustaining a Complete Anterior Cruciate Ligament Tear in Early Adulthood. *Arthritis Care Res (Hoboken)* 69:201-208.
7. Bannwarth B, Kostine M. 2014. Targeting nerve growth factor (NGF) for pain management: what does the future hold for NGF antagonists? *Drugs* 74:619-626.
8. Holmes D. 2012. Anti-NGF painkillers back on track? *Nature reviews Drug discovery* 11:337-338.
9. Jay GD, Fleming BC, Watkins BA, et al. 2010. Prevention of cartilage degeneration and restoration of chondroprotection by lubricin tribosupplementation in the rat following anterior cruciate ligament transection. *Arthritis Rheum* 62:2382-2391.
10. Jay GD, Elsaid KA, Kelly KA, et al. 2012. Prevention of cartilage degeneration and gait asymmetry by lubricin tribosupplementation in the rat following anterior cruciate ligament transection. *Arthritis Rheum* 64:1162-1171.
11. Flannery CR, Zollner R, Corcoran C, et al. 2009. Prevention of cartilage degeneration in a rat model of osteoarthritis by intraarticular treatment with recombinant lubricin. *Arthritis Rheum* 60:840-847.
12. Waller KA, Chin KE, Jay GD, et al. 2017. Intra-articular Recombinant Human Proteoglycan 4 Mitigates Cartilage Damage After Destabilization of the Medial Meniscus in the Yucatan Minipig. *Am J Sports Med* 45:1512-1521.
13. Lawrence A, Xu X, Bible MD, et al. 2015. Synthesis and characterization of a lubricin mimic (mLub) to reduce friction and adhesion on the articular cartilage surface. *Biomaterials* 73:42-50.
14. Andresen Eguiluz RC, Cook SG, Tan M, et al. 2017. Synergistic Interactions of a Synthetic Lubricin-Mimetic with Fibronectin for Enhanced Wear Protection. *Frontiers in bioengineering and biotechnology* 5:36.
15. Jones AR, Flannery CR. 2007. Bioregulation of lubricin expression by growth factors and cytokines. *Eur Cell Mater* 13:40-45; discussion 45.
16. DuRaine G, Neu CP, Chan SM, et al. 2009. Regulation of the friction coefficient of articular cartilage by TGF-beta1 and IL-1beta. *J Orthop Res* 27:249-256.
17. Elsaid KA, Zhang L, Waller K, et al. 2012. The impact of forced joint exercise on lubricin biosynthesis from articular cartilage following ACL transection and intra-articular lubricin's effect in exercised joints following ACL transection. *Osteoarthritis Cartilage*

- 20:940-948.
18. Teeple E, Elsaid KA, Jay GD, et al. 2011. Effects of supplemental intra-articular lubricin and hyaluronic acid on the progression of posttraumatic arthritis in the anterior cruciate ligament-deficient rat knee. *Am J Sports Med* 39:164-172.
 19. Ruan MZ, Erez A, Guse K, et al. 2013. Proteoglycan 4 expression protects against the development of osteoarthritis. *Sci Transl Med* 5:176ra134.
 20. Waller KA, Zhang LX, Elsaid KA, et al. 2013. Role of lubricin and boundary lubrication in the prevention of chondrocyte apoptosis. *Proc Natl Acad Sci U S A* 110:5852-5857.
 21. Bonnevie ED, Delco ML, Bartell LR, et al. 2018. Microscale frictional strains determine chondrocyte fate in loaded cartilage. *J Biomech* 74:72-78.
 22. Jay GD, Torres JR, Rhee DK, et al. 2007. Association between friction and wear in diarthrodial joints lacking lubricin. *Arthritis Rheum* 56:3662-3669.
 23. Karamchedu NP, Tofte JN, Waller KA, et al. 2015. Superficial zone cellularity is deficient in mice lacking lubricin: a stereoscopic analysis. *Arthritis Res Ther* 18:64.
 24. Vugmeyster Y, Wang Q, Xu X, et al. 2012. Disposition of human recombinant lubricin in naive rats and in a rat model of post-traumatic arthritis after intra-articular or intravenous administration. *AAPS J* 14:97-104.
 25. Larson KM, Zhang L, Elsaid KA, et al. 2017. Reduction of friction by recombinant human proteoglycan 4 in IL-1alpha stimulated bovine cartilage explants. *J Orthop Res* 35:580-589.
 26. Hurtig M, Drangova, M., Holdsworth, D. 2016. Allometric Scaling for Implementation of Sustained Release Intra-Articular Medications - A Pilot Study. OARSI World Congress on Osteoarthritis. Amsterdam, Netherlands. *Osteoarthritis Cartilage* 24:S529-S530.
 27. Elsaid KA, Fleming BC, Oksendahl HL, et al. 2008. Decreased lubricin concentrations and markers of joint inflammation in synovial fluids from patients with anterior cruciate ligament injury. *Arthritis Rheum* 58:1707-1715.
 28. Lattermann C, Jacobs CA, Proffitt Bunnell M, et al. 2017. A Multicenter Study of Early Anti-inflammatory Treatment in Patients With Acute Anterior Cruciate Ligament Tear. *Am J Sports Med* 45:325-333.
 29. Abubacker S, Dorosz SG, Ponjevic D, et al. 2016. Full-Length Recombinant Human Proteoglycan 4 Interacts with Hyaluronan to Provide Cartilage Boundary Lubrication. *Ann Biomed Eng* 44:1128-1137.
 30. Samsom M, Iwabuchi Y, Sheardown H, et al. 2017. Proteoglycan 4 and hyaluronan as boundary lubricants for model contact lens hydrogels. *J Biomed Mater Res B Appl Biomater*.
 31. Ai M, Cui Y, Sy MS, et al. 2015. Anti-lubricin monoclonal antibodies created using lubricin-knockout mice immunodetect lubricin in several species and in patients with healthy and diseased joints. *PLoS One* 10:e0116237.
 32. Steele MA, Garcia F, Lowerison M, et al. 2014. Technical note: Three-dimensional imaging of rumen tissue for morphometric analysis using micro-computed tomography. *Journal of dairy science* 97:7691-7696.
 33. Rhee DK, Marcelino J, Baker M, et al. 2005. The secreted glycoprotein lubricin protects cartilage surfaces and inhibits synovial cell overgrowth. *J Clin Invest* 115:622-631.
 34. Aninwene GE, 2nd, Yang Z, Ravi V, et al. 2014. Lubricin as a novel nanostructured protein coating to reduce fibroblast density. *International journal of nanomedicine* 9:3131-3135.
 35. Greene GW, Martin LL, Tabor RF, et al. 2015. Lubricin: a versatile, biological anti-

- adhesive with properties comparable to polyethylene glycol. *Biomaterials* 53:127-136.
36. Greene GW, Duffy E, Shalhan A, et al. 2016. Electrokinetic Properties of Lubricin Antiadhesive Coatings in Microfluidic Systems. *Langmuir* 32:1899-1908.
 37. Zappone B, Ruths M, Greene GW, et al. 2007. Adsorption, lubrication, and wear of lubricin on model surfaces: polymer brush-like behavior of a glycoprotein. *Biophys J* 92:1693-1708.
 38. Zappone B, Greene GW, Oroudjev E, et al. 2008. Molecular aspects of boundary lubrication by human lubricin: effect of disulfide bonds and enzymatic digestion. *Langmuir* 24:1495-1508.
 39. Yu J, Banquy X, Greene GW, et al. 2012. The boundary lubrication of chemically grafted and cross-linked hyaluronic acid in phosphate buffered saline and lipid solutions measured by the surface forces apparatus. *Langmuir* 28:2244-2250.
 40. Jay GD, Harris DA, Cha CJ. 2001. Boundary lubrication by lubricin is mediated by O-linked beta(1-3)Gal-GalNAc oligosaccharides. *Glycoconjugate J* 18:807-815.
 41. Estrella RP, Whitelock JM, Packer NH, et al. 2010. The glycosylation of human synovial lubricin: implications for its role in inflammation. *Biochem J* 429:359-367.
 42. Chang DP, Abu-Lail NI, Guilak F, et al. 2008. Conformational mechanics, adsorption, and normal force interactions of lubricin and hyaluronic acid on model surfaces. *Langmuir* 24:1183-1193.
 43. Jay GD. 1992. Characterization of a bovine synovial fluid lubricating factor. I. Chemical, surface activity and lubricating properties. *Connect Tissue Res* 28:71-88.
 44. Nugent-Derfus GE, Chan AH, Schumacher BL, et al. 2007. PRG4 exchange between the articular cartilage surface and synovial fluid. *J Orthop Res* 25:1269-1276.
 45. Nugent GE, Aneloski NM, Schmidt TA, et al. 2006. Dynamic shear stimulation of bovine cartilage biosynthesis of proteoglycan 4. *Arthritis Rheum* 54:1888-1896.
 46. Andriacchi TP, Briant PL, Bevill SL, et al. 2006. Rotational Changes at the Knee after ACL Injury Cause Cartilage Thinning. *Clin Orthop Relat Res* 442:39-44.
 47. Ballard BL, Antonacci JM, Temple-Wong MM, et al. 2012. Effect of tibial plateau fracture on lubrication function and composition of synovial fluid. *J Bone Joint Surg Am* 94:e64.
 48. Larson KM, Zhang L, Badger GJ, et al. 2017. Early genetic restoration of lubricin expression in transgenic mice mitigates chondrocyte peroxynitrite release and caspase-3 activation. *Osteoarthritis Cartilage* 25:1488-1495.
 49. Ni GX, Lei L, Zhou YZ. 2012. Intensity-dependent effect of treadmill running on lubricin metabolism of rat articular cartilage. *Arthritis Res Ther* 14:R256.
 50. Grad S, Lee CR, Wimmer MA, et al. 2006. Chondrocyte gene expression under applied surface motion. *Biorheol* 43:259-269.
 51. Schatti OR, Markova M, Torzilli PA, et al. 2015. Mechanical Loading of Cartilage Explants with Compression and Sliding Motion Modulates Gene Expression of Lubricin and Catabolic Enzymes. *Cartilage* 6:185-193.
 52. Alquraini A, Garguilo S, D'Souza G, et al. 2015. The interaction of lubricin/proteoglycan 4 (PRG4) with toll-like receptors 2 and 4: an anti-inflammatory role of PRG4 in synovial fluid. *Arthritis Res Ther* 17:353.
 53. Iqbal SM, Leonard C, Regmi SC, et al. 2016. Lubricin/Proteoglycan 4 binds to and regulates the activity of Toll-Like Receptors In Vitro. *Scientific reports* 6:18910.
 54. Eckstein F, Winzheimer M, Hohe J, et al. 2001. Interindividual variability and correlation among morphological parameters of knee joint cartilage plates: analysis with three-

- dimensional MR imaging. *Osteoarthritis Cartilage* 9:101-111.
55. Davies DV. 1946. Synovial membrane and synovial fluid of joints. *Lancet* 2:815-819.
 56. Blewis ME, Schumacher BL, Klein TJ, et al. 2007. Microenvironment regulation of PRG4 phenotype of chondrocytes. *J Orthop Res* 25:685-695.
 57. Das S, Banquy X, Zappone B, et al. 2013. Synergistic interactions between grafted hyaluronic acid and lubricin provide enhanced wear protection and lubrication. *Biomacromolecules* 14:1669-1677.
 58. Chang DP, Abu-Lail NI, Coles JM, et al. 2009. Friction force microscopy of lubricin and hyaluronic acid between hydrophobic and hydrophilic surfaces. *Soft Matter* 5:3438-3445.
 59. Bonnevie ED, Galesso D, Secchieri C, et al. 2015. Elastoviscous Transitions of Articular Cartilage Reveal a Mechanism of Synergy between Lubricin and Hyaluronic Acid. *PLoS One* 10:e0143415.
 60. Zhao C, Ozasa Y, Shimura H, et al. 2016. Effects of lubricant and autologous bone marrow stromal cell augmentation on immobilized flexor tendon repairs. *J Orthop Res* 34:154-160.
 61. Teeple E, Karamchedu NP, Larson KM, et al. 2016. Arthroscopic irrigation of the bovine stifle joint increases cartilage surface friction and decreases superficial zone lubricin. *J Biomech* 49:3106-3110.
 62. Reesink HL, Watts AE, Mohammed HO, et al. 2017. Lubricin/proteoglycan 4 increases in both experimental and naturally occurring equine osteoarthritis. *Osteoarthritis Cartilage* 25:128-137.

Acknowledgments: NIH R01AR067748, PR110746, R42AR057276, CDMRP PR110746, and
Lubris, LLC.

Conflicts of Interest: G.D.J. and T.A.S. own equity in Lubris BioPharma and have licensed
patents related to the use of rhPRG4. T.S. also consults for Lubris BioPharma.

Accepted Article

Legends

Figure 1. Timeline of Yucatan mini-pig pharmacokinetic (PK) study of intra-articular (IA) I^{131} -rhPRG4 at Day 0 (D0) following ACL transection 5 days prior (D-5). The remaining number of porcine following each tissue harvest time point is illustrated. The first harvest involving 5 animals occurred at 10 mins following IA (D0+10m) which served as time zero in PK calculations. Sequential tissue harvests following IA were conducted at 24 hrs (D1), 72 hrs (D2), 6 days (D6), 13 days (D13) and 20 days (D20). At each time point synovium and cartilage collected from each joint compartment and both condyles were weighed and counted for radioactivity across 21 animals. Samples of SF, blood, liver and proximal lymph node were also collected and counted. Three animals were removed from the analysis as they did not receive IA injection correctly and demonstrated very high lymph node radioactivity.

Figure 2. Cartilage surface area and volume analysis by microCT. Four previously frozen unoperated Yucatan mini-pig left knee joints served as controls to determine the surface area and volume of each cartilage surface from the patellofemoral joint and both compartments of the tibiofemoral joint. The product of the tissue density multiplied by the representative cartilage volume from each area was used as the tissue mass denominator in normalizing gamma counts per tissue weight to determine the total amount of I^{131} -rhPRG4 resident in each cartilage surface. Mean \pm SD is reported.

Figure 3. Least squares fitting model and Akaike Information Criterion (AIC) of the percent of total dose of I^{131} -rhPRG4 in recovered knee tissue counts including lavage and aspirated SF across time points at 10 minutes, days 1,3,6,13 and 20 for 18 porcine following intra-articular I^{131} -rhPRG4 delivered 5 days after ACL transection. A) 98% of the total dose at 10 minutes (day 0) was accounted for across the 6 time points by least squares elimination profile which did not conform to a predicted AIC two-compartment model. B) 33% of the total dose at 10 minutes was accounted for by considering only knee tissue counts (excluding lavage and aspirated SF) which conformed to an AIC two-compartment model. D) Akaike Information Criterion parameter tables showing AIC $t_{1/2}$ estimates in days, and coefficient of variation (CV%). Error bars are mean \pm SE; N=3 at each sampling time.

Figure 4. Knee joint tissue concentrations of I^{131} -rhPRG4 at 10 minutes (day 0), days 1 and 3 (A), and days 6,13 and 20 (B). Tibial cartilage and synovial membrane surfaces appeared to contain relatively larger amounts of I^{131} -rhPRG4 at 10 minutes and remained greater by days 1,3 and 6 for

synovial surfaces. By day 13 and 20, cartilage surfaces showed greater relative amounts of I¹³¹-rhPRG4. Abbreviations: Medial femoral condyle (MFC), medial tibial plateau (MTP), lateral femoral condyle (LFC), lateral tibial plateau (LTP), medial meniscus (MM), lateral meniscus (LM), synovial membrane anterior compartment (SMAC) and synovial membrane posterior compartment (SMPC). Error bars are mean ± SE; N=3 at each sampling time.

Figure 5. Percent of recovered total knee I¹³¹-rhPRG4 across time points at 10 minutes (day 0), days 1,3,6,13 and 20 in 18 porcine following intra-articular I¹³¹-rhPRG4 delivered 5 days after ACL transection. (A) Comparison of total femoral and tibial cartilage and (B) total medial and lateral cartilage. Initially I¹³¹-rhPRG4 localized more to the medial joint compartment and tibial cartilage surfaces. Towards the end of the concentration-time profiles studied at day 20, the lateral joint compartment and femoral cartilage retained a greater relative percentage of recoverable I¹³¹-rhPRG4. Error bars are mean ± SE; N=3 at each sampling time.

Figure 6. Densitometry of rhPRG4 (MW~300 kDa) and native porcine PRG4 (MW~180 kDa) bands on Western blots of joint surface lavage in 12 of the 18 porcine following intra-articular I¹³¹-rhPRG4 delivered 5 days after ACL transection. A) Samples at 10 minutes (day 0) (N=3), 1 (N=3), 3 (N=2), 6 (N=1), 13 (N=2) and 20 (N=1) were analyzed on SDS-PAGE and transferred to nitrocellulose 4 months following recovery to allow sufficient radioactive decay. Blots were probed with polyclonal antibody 1752 and densitometry was performed in triplicate and normalized against a 10 µg/ml preparation of rhPRG4. B) rhPRG4 decreased over time and was detectable up to 13 days later, whereas porcine PRG4 increased over that same interval. Error bars are mean ± SD.

Figure 7. Immunohistochemistry of total PRG4 comprising injected rhPRG4 and native PRG4 across representative porcine at 10 minutes (day 0), days 1,3,6,13 and 20 following intra-articular I¹³¹-rhPRG4 delivered 5 days after ACL transection in 18 porcine. Cartilage surface immunoprobings with monoclonal antibody 9G3 was counterstained with DAPI in sections from the two apposing surfaces from medial and lateral joint compartments. Cartilage surface staining was qualitatively most intense at day 1 and 3, and least intense by day 20 which is similar to untreated and historical control porcine cartilage. Chondrocyte positivity for PRG4 (white arrows) appeared most intense at day 6 and may be indicative of renewed native expression of porcine PRG4.

Table 1. Summary of Fitted Two Compartment Model by Tissue and Fluid Type

Tissue(s) and/or Synovial Fluid or Lavage	$t_{1/2,\alpha}$ (Days)	$t_{1/2,\beta}$ (Days)	K12 (Day ⁻¹)	K21 (Day ⁻¹)
Synovial Fluid	0.26	28.07	0.034	0.062
Anterior & Posterior Synovium	0.59	3.09	0.104	0.253
Cartilage + Meniscii	0.36	7.10	0.443	0.149
Cartilage + Meniscii + Cartilage Lavage	0.22	6.19	0.450	0.130
Cartilage + Meniscii + Cartilage Lavage + Anterior & Posterior Synovium	0.33	4.40	0.299	0.186
Cartilage + Meniscii + Anterior & Posterior Synovium	0.47	4.81	0.252	0.179

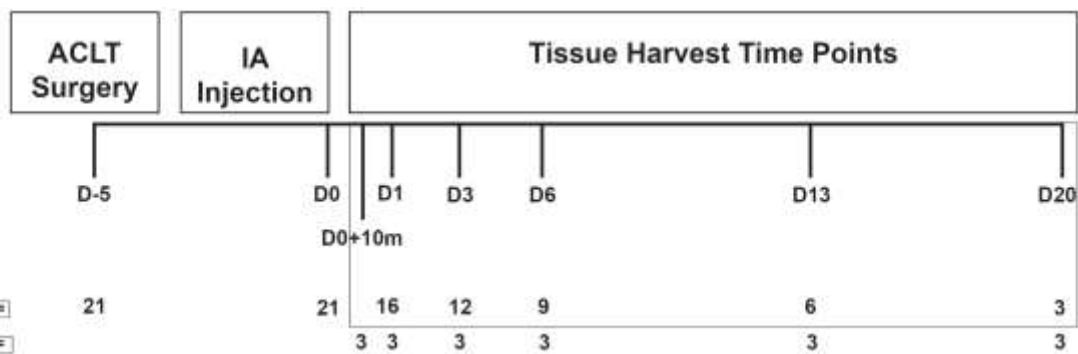


Figure 1



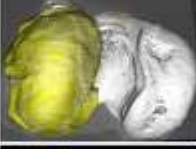



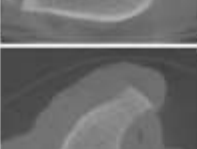

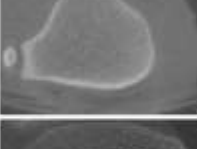
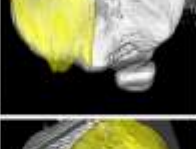
	CT Image	Cartilage Reconstruction	Surface Area (mm ²)	Volume (mm ³)	Tissue Weight Denominator (g)
MFC			1255.0 ± 199.7	613.8 ± 100.7	0.614
LFC			1274.3 ± 125.4	578.1 ± 71.5	0.578
TRO			1733.6 ± 39.7	734.1 ± 23.6	0.734
MTP			763.5 ± 31.2	258.6 ± 36.0	0.259
LTP			988.3 ± 427.3	300.1 ± 100.6	0.300
PAT			702.8 ± 95.6	318.6 ± 39.6	0.319
MM			—	—	1.94
LM			—	—	1.98
SYN			—	—	4.00

Figure 2

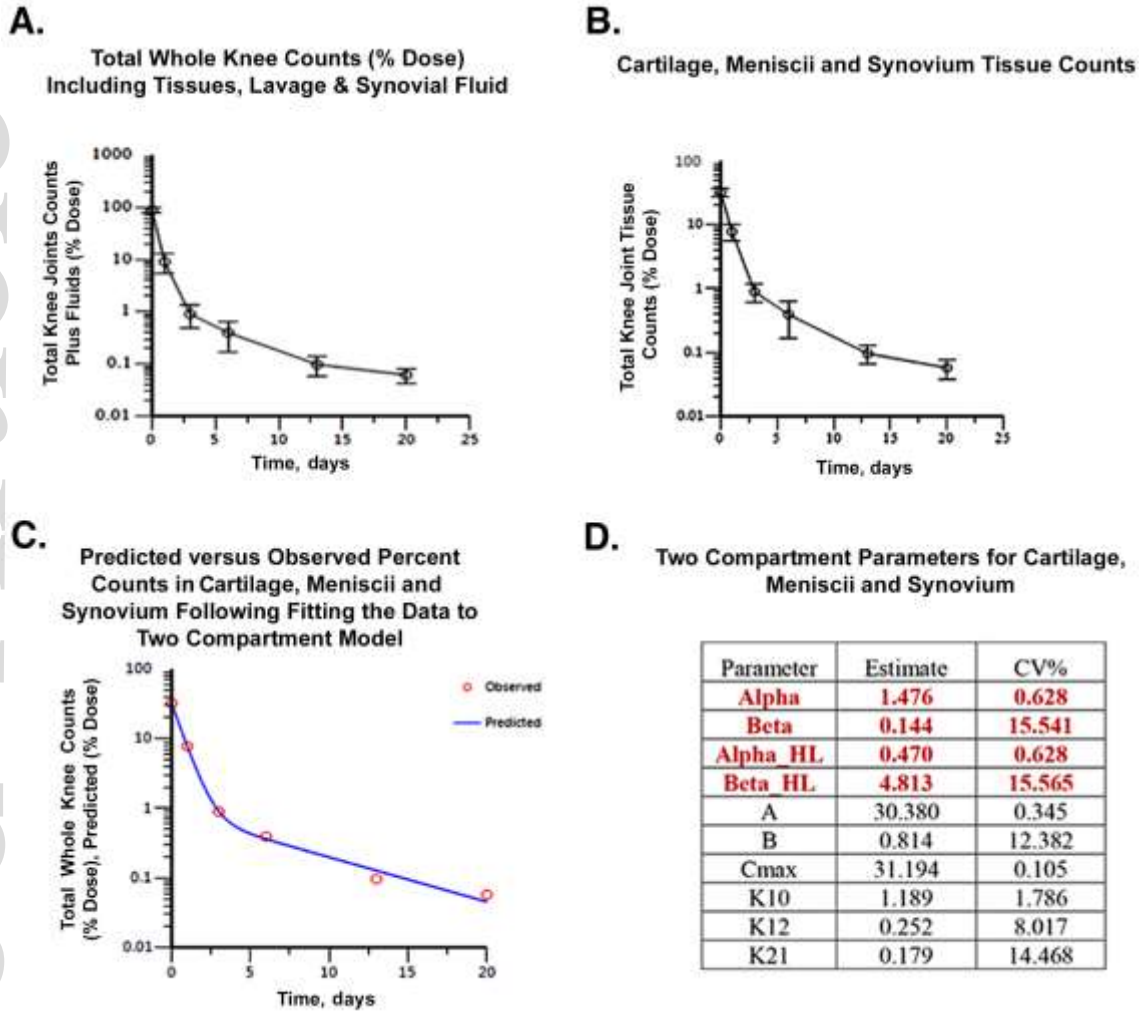


Figure 3

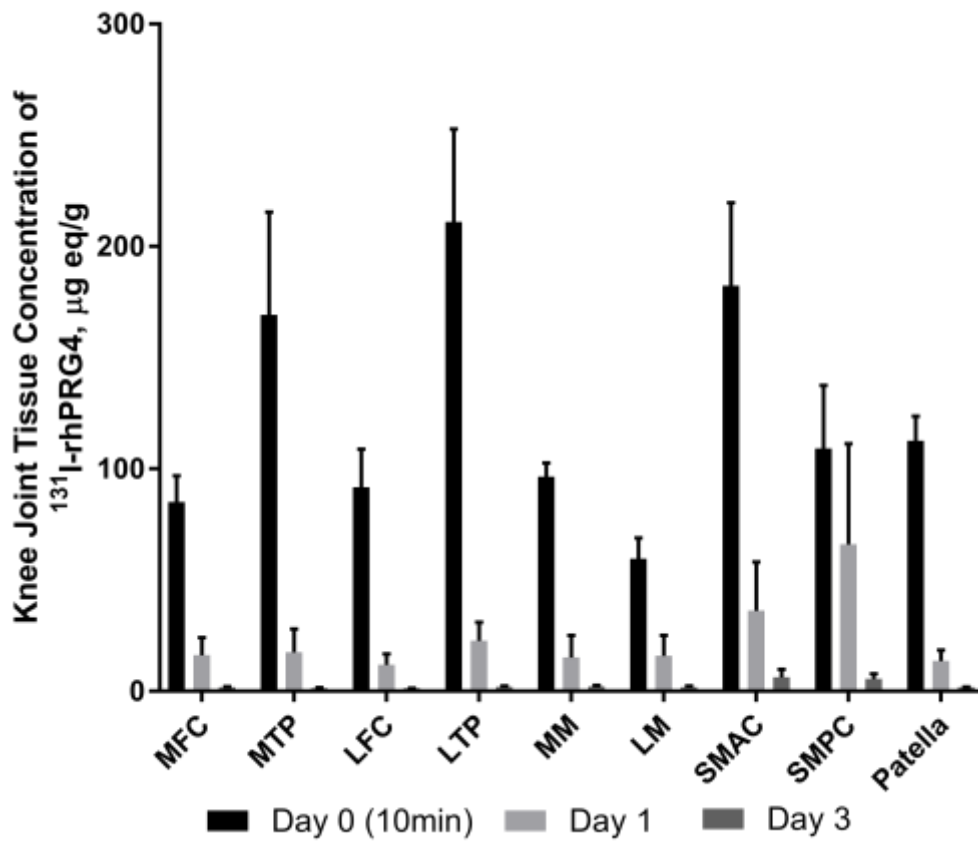


Figure 4 (A)

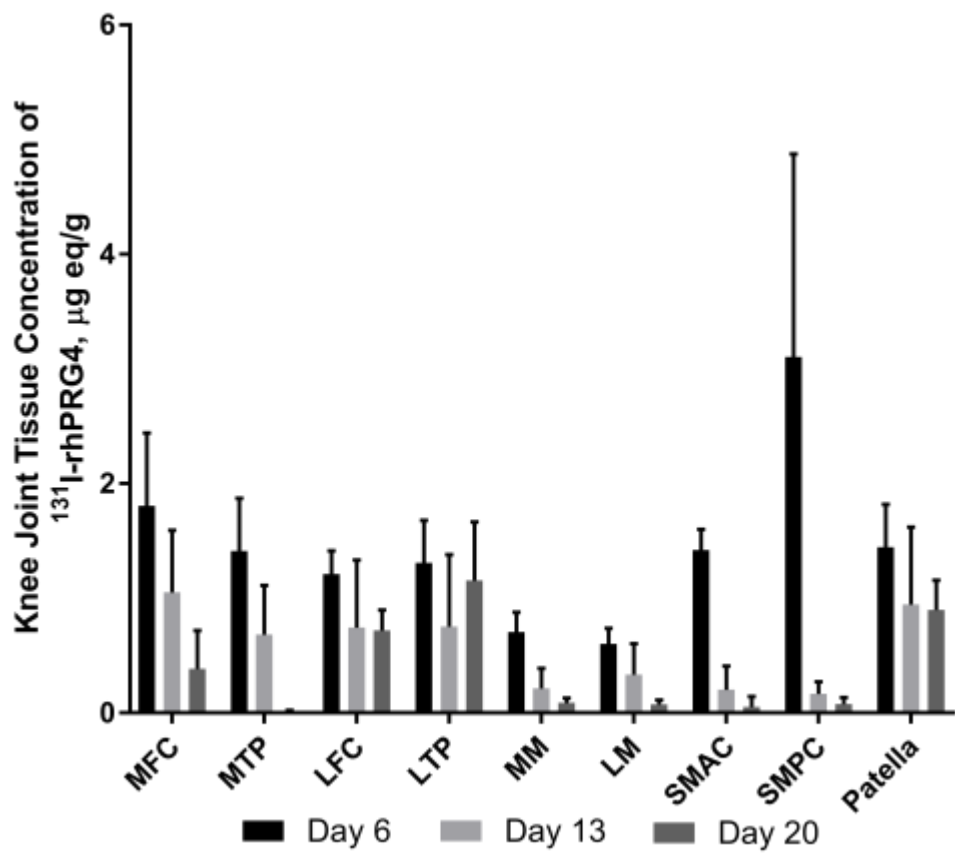


Figure 4(B)

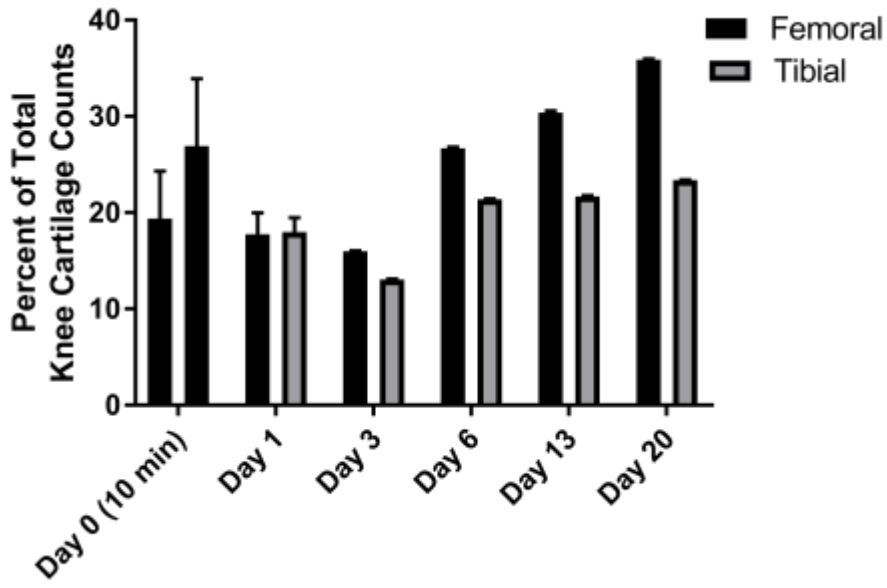


Figure 5(A)

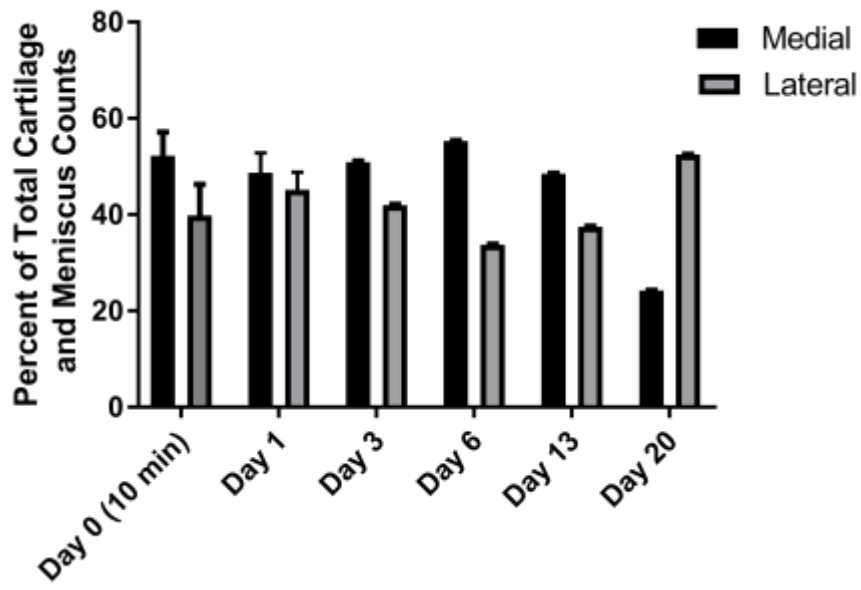


Figure 5(B)

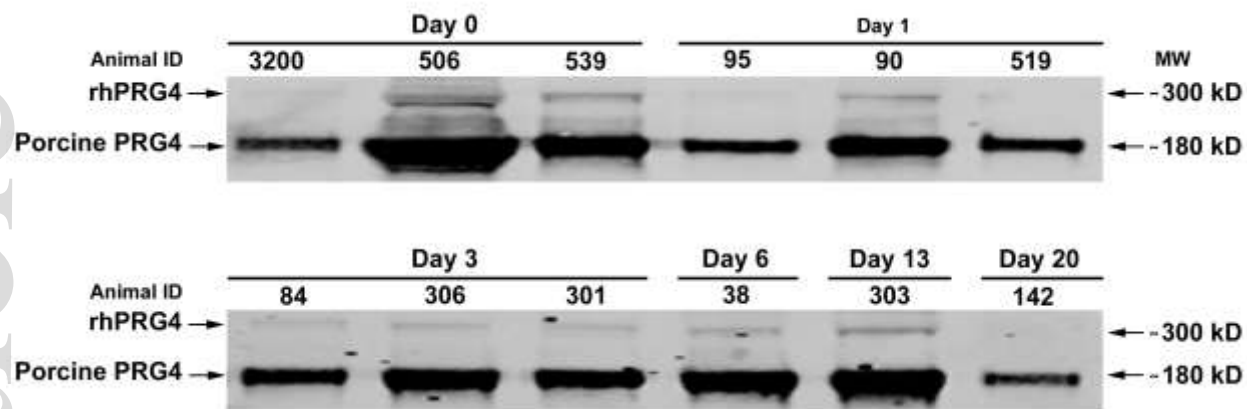


Figure 6(A)

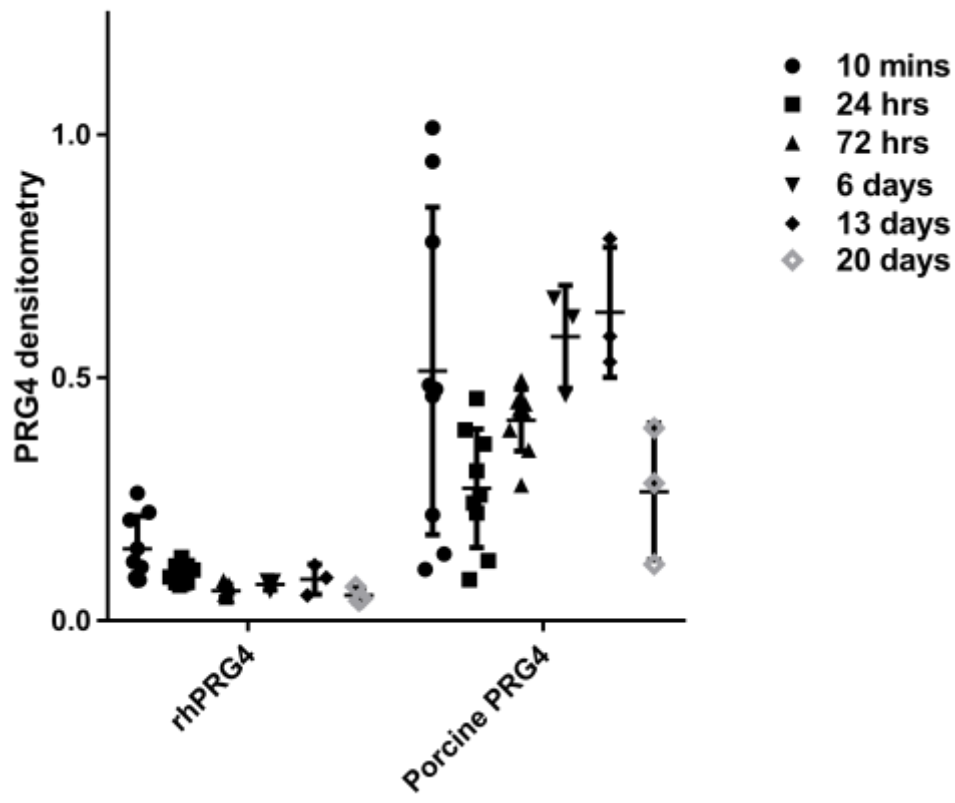


Figure 6(B)

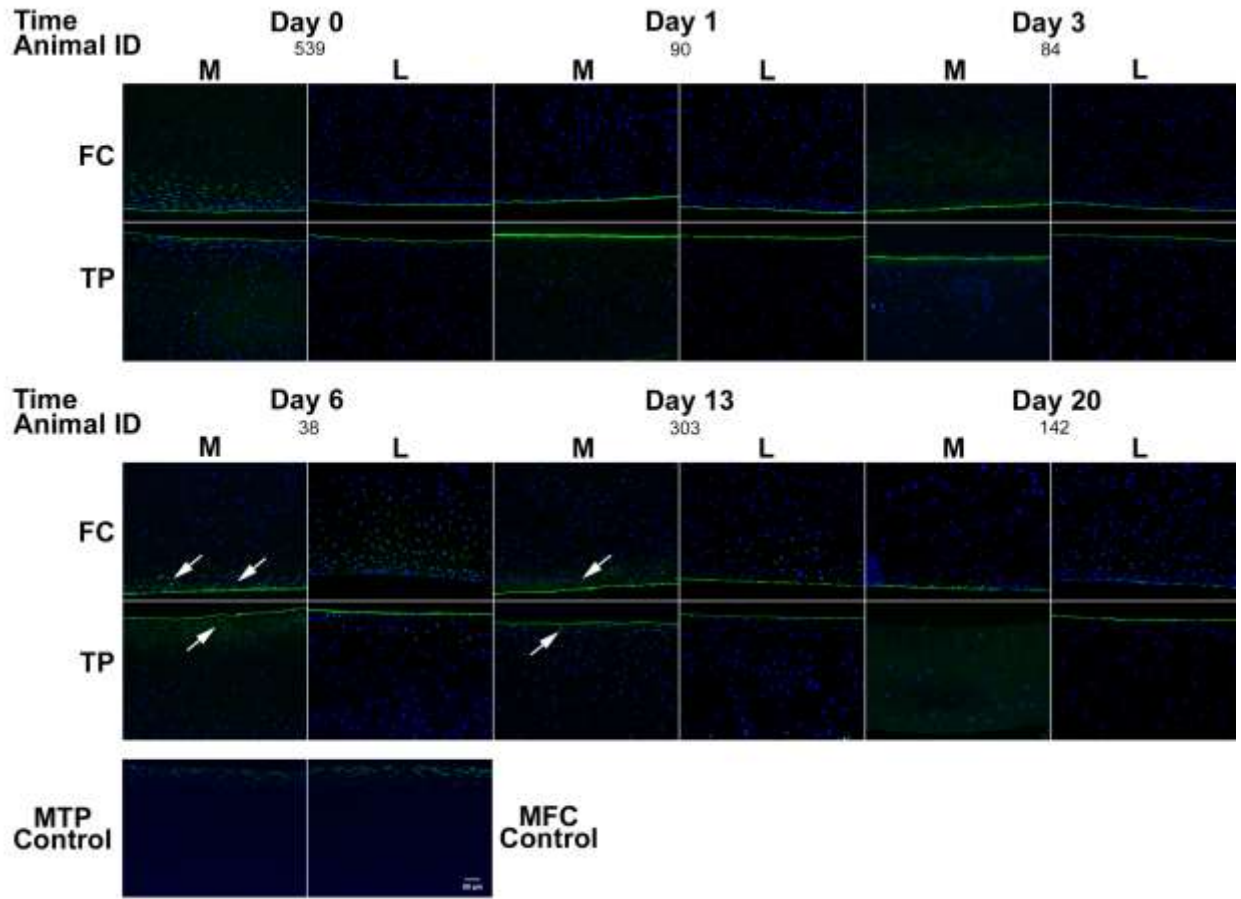


Figure 7